

## Toward the Ultra-incompressible Carbon Materials. Computational Simulation and Experimental Observation

Yu. A. Kvashnina,<sup>†,‡</sup> A. G. Kvashnin,<sup>†,‡</sup> M. Yu. Popov,<sup>†,‡,§</sup> B. A. Kulnitskiy,<sup>†,‡</sup> I. A. Perezhogin,<sup>†,‡</sup>  
 E. V. Tyukalova,<sup>†,‡</sup> L. A. Chernozatonskii,<sup>||</sup> P. B. Sorokin,<sup>\*,†,‡,§</sup> and V. D. Blank<sup>†,‡,§</sup>

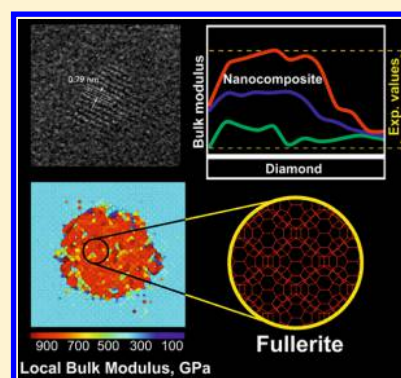
<sup>†</sup>Technological Institute for Superhard and Novel Carbon Materials, 7a Centralnaya Street, Troitsk, Moscow, 142190, Russian Federation

<sup>‡</sup>Moscow Institute of Physics and Technology, 9 Institutsky lane, Dolgoprudny, 141700, Russian Federation

<sup>§</sup>National University of Science and Technology MISiS, 4 Leninskiy prospekt, Moscow, 119049, Russian Federation

<sup>||</sup>Emanuel Institute of Biochemical Physics, 4 Kosigina Street, Moscow, 119334, Russian Federation

**ABSTRACT:** The common opinion that diamond is the stiffest material is disproved by a number of experimental studies where the fabrication of carbon materials based on polymerized fullerenes with outstanding mechanical stiffness was reported. Here we investigated the nature of this unusual effect. We present a model constituted of compressed polymerized fullerite clusters implemented in a diamond matrix with bulk modulus  $B_0$  much higher than that of diamond. The calculated  $B_0$  value depends on the sizes of both fullerite grain and diamond environment and shows close correspondence with measured data. Additionally, we provide results of experimental study of atomic structure and mechanical properties of ultrahard carbon material supported the presented model.



The leading position of diamond as the hardest material was challenged by a number of experimental results where synthesis of amorphous carbon with superior mechanical properties was reported.<sup>1,2</sup> The measurements have shown that obtained material displayed a disordered structure and consisted of the polymerized  $C_{60}$  fullerenes with hardness and bulk modulus significantly exceeding the corresponding characteristics of diamond. These results were unusual because it is well-known that polymerized fullerite displays low stiffness, which was clearly shown in various theoretical studies.<sup>3–7</sup>

An obtained sample of ultrahard carbon scratched the (111) surface of diamond, which is the hardest diamond surface (the hardness is  $167 \pm 5$  GPa<sup>8</sup>). Depending on the synthesis conditions, the bulk modulus of such material varied from 540 to 1700 GPa, and the hardness varied from 150 to 300 GPa.<sup>8</sup> For comparison, the bulk modulus of a single-crystal diamond equals 442 GPa.<sup>9</sup>

The discrepancy between theory and experiment suggests the specific mechanism of the fullerite stiffening during its polymerization. The theoretical analysis made by Chernozatonskii et al.<sup>10</sup> showed that the model of a new three-dimensional polymerized fullerite corresponded with the experimental data by X-ray diffraction<sup>2,8</sup> and should have lower lattice parameter than the relaxed structure. Nevertheless, this data allows one to conclude that the increasing rigidity of a polymerized fullerite is originated from the mechanical strain induced by the surrounding carbon material.

In the present paper, we report the model consisting of the compressed polymerized fullerite clusters embedded in a diamond matrix. We investigated in detail the atomic structure of such carbon nanocomposite and compared it with our experimental data. We calculated the bulk modulus of the proposed structure depending on the sizes of both fullerite grain and diamond environment and showed its close correspondence with the measured bulk modulus of ultrahard fullerite. We explained the nature of ultra-incompressibility of this unique material by analysis of its atomic structure and distribution of atom-projected bulk moduli.

We investigated the effect of stiffening of polymerized fullerenes by considering the model of a compressed fullerite grain embedded in a single-crystal diamond matrix as shown in Figure 1a. After geometry optimization, the resulting structure of nanocomposite is under normal pressure conditions but with the compressed grain, the dilatation of which is prevented by surrounded diamond matrix.

In this work, we characterized the mechanical properties of the considered structures by investigation of their bulk moduli  $B_0$ . The bulk modulus describes the ability of an object to change its volume under the influence of uniform hydrostatic compression. To obtain the energy versus volume curve required for bulk modulus calculations, each considered

Received: April 10, 2015

Accepted: May 20, 2015

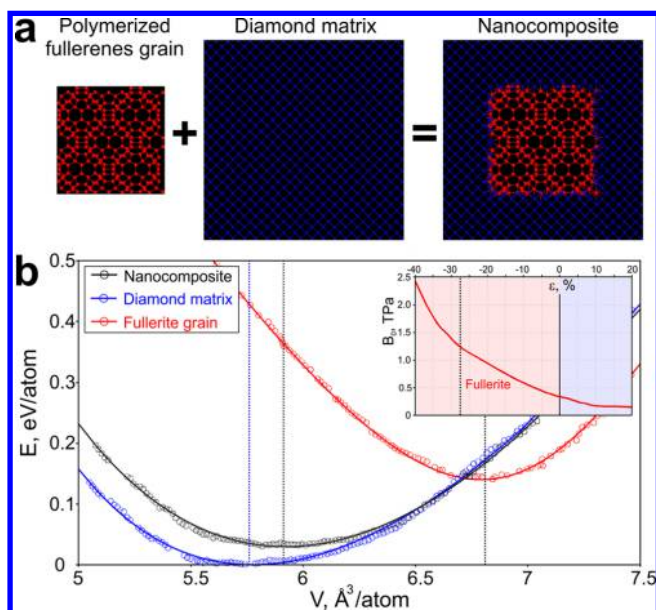


**Figure 1.** (a) The atomic structure of the proposed model of ultrastiff carbon nanocomposite; (b) strain energy of nanocomposite and its component parts (fullerite grain, diamond matrix) depending on unit volume. In the inset, the dependence of bulk modulus ( $B_0$ ) of polymerized fullerite on the uniform strain ( $\epsilon$ ) is presented.

structure was hydrostatically compressed and expanded; at each step, the optimization of geometry was carried out. Based on the calculated data, the energy of each investigated structure

depending on the unit volume was evaluated, and the bulk modulus of all considered structures was found by the method of approximation using the Murnaghan equation.<sup>11</sup>

We considered the model of fullerite proposed by O’Keeffe<sup>12</sup> made by (6 + 6) cycloaddition process, which led to the formation of the whole  $sp^3$ -hybridized structure. It can be speculated that O’Keeffe’s polymerized fullerite structure can be formed from the previously considered fullerene polymer<sup>10</sup> (which corresponded well with the X-ray diffraction data). The latter structure has orthorhombic symmetry in which fullerenes connect with each other by (2 + 2) cycloaddition. The growing pressure can lead to changing of (2 + 2) to (3 + 3) and further to (6 + 6) cycloaddition by reconstruction of connected hexagonal rings.

O’Keeffe’s model displays a relatively high bulk modulus (369.7 GPa<sup>4</sup>) with respect to other polymerized fullerite models,<sup>3,4,7</sup> which nevertheless is lower than diamond  $B_0$ . However, compression of the material leads to its stiffening represented by an increase in the sound velocities values with increasing pressure.<sup>8,13</sup> We calculated the dependence of bulk modulus of polymerized fullerite on the uniform strain (see Figure 1b, inset). We found that  $B_0$  of the structure varies from 120 to 2450 GPa in the deformation range from 20% to –40% due to the anharmonic terms inclusion to the linear elastic constant.

The localized character of C–C bonds in the structure allows us to decompose the strain energy of the total nanocomposite to the strain energies of the component parts (fullerite grain, diamond matrix), and their dependences on the corresponding unit volumes are presented in Figure 1b. At the equilibrium

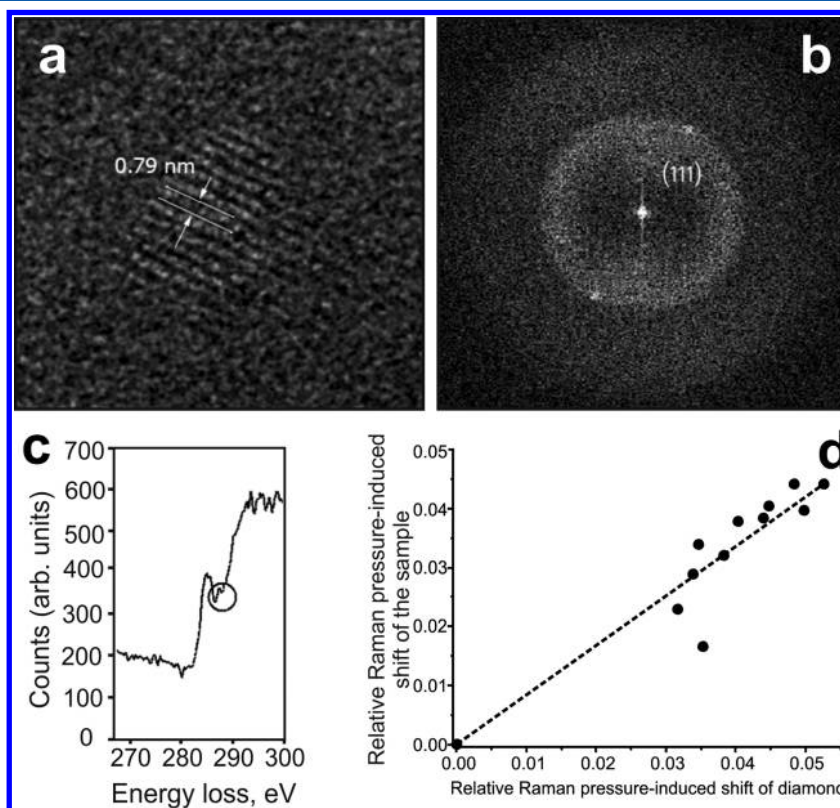


**Figure 2.** A high-resolution image (a) and a Fourier transformation (b) of elements of the combined amorphous–crystalline structure in the ultrahard fullerite sample, fragment of EELS spectrum (c), where the region marked by a circle indicates that fullerenes maintain its atomic structure in the material; (d) dependencies of the relative Raman pressure-induced shifts  $(\omega - \omega_0)/\omega_0$  against the relative diamond Raman pressure-induced shift of the centroid (determined by a singlet and a doublet modes of the stressed diamond anvil).

state of nanocomposite (dark vertical line in Figure 1b), the fullerite grain is in compressed and therefore stiffened state. According to this, the main feature of the proposed model of ultrastiff carbon nanocomposite is that fullerite grains are hydrostatically compressed and then incorporated into a diamond matrix, which could be formed under the specific conditions of a 12–14 GPa pressure and a  $\sim 1400$  K temperature from  $C_{60}$  fullerite treatment.<sup>14</sup> The surrounding diamond prevents relaxation of the stressed grain and the resulting relaxed nanocomposite consists of strained but mutually balanced parts. Such compression will lead to an increase in the density of the grain from  $3.06 \text{ g/cm}^3$  (uncompressed fullerite) to  $4.98 \text{ g/cm}^3$  (compression of 40%), while the density of diamond is  $3.55 \text{ g/cm}^3$ . Keeping in mind the strong dependence of  $B_0$  on the compression of fullerite (Figure 1b), it can be concluded that the bulk modulus value of the resulting nanocomposite can exceed the bulk modulus of a single-crystal diamond.

The theoretical model correlates well with obtained experimental data. In general, the structure of ultrahard fullerite samples can be represented as a combined amorphous–crystalline<sup>8</sup> and depends on the pressure–temperature synthesis conditions. In particular, at temperatures below 1300 K the crystalline structure according to a TEM study shows a sequence of FCC-phases explained by a bonded  $C_{60}$  chains formation. We would mention here that the range of the bulk modulus from 540 to 1700 GPa is attributed to the different sets of structures of the fullerite.

We observed the perturbed cubic structures with the interplane distance  $d_{111} = 0.32\text{--}0.34 \text{ nm}$ , which means the lattice parameter is close to  $a_0 = 0.59 \text{ nm}$ . In addition to the above fragments, a TEM study shows the presence of elements of the combined amorphous–crystalline structure in the sample. An example of the particular element is given in Figure 2 where a fragment of a crystal structure in the amorphous matrix and the corresponding Fourier transformation are shown in Figure 2a,b, respectively. Also, the fragment of EELS spectra near the K-edge of carbon is shown in Figure 2c. One of the most characteristic peaks that correspond to the fullerene molecules is highlighted by a circle. Reflexes from Figure 2b correspond to the series of fringes that are clearly seen in Figure 2a. The interplanar distance of the fullerite crystalline is  $d_{111} \approx 0.79 \text{ nm}$ , which corresponds to a slightly disturbed lattice parameter of  $C_{60}$  ( $a_0 \approx 1.36 \text{ nm}$ ).

For the present study, we selected the ultrahard fullerite obtained under conditions that permit the *in situ* control of fullerite transformations during the synthesis. The ultrahard fullerite was synthesized at a pressure above 18 GPa at room temperature under conditions of a large shear deformation using diamond anvil cell. We loaded the sample of  $C_{60}$  to an 18–19 GPa pressure. After applying of shear deformation, an effect of pressure self-multiplication<sup>8</sup> (due to the elastic moduli jump) is observed. As a result, the pressure in the sample increased to 25–30 GPa. The Raman spectra of ultrahard fullerite are composed of two broad bands around  $1550 \text{ cm}^{-1}$  (a result of broadening and overlapping of the  $C_{60}$  tangential modes) and around  $500 \text{ cm}^{-1}$  (a result of broadening and overlapping of the  $C_{60}$  intermediate modes). The bulk modulus was calculated from the dependency of the tangential Raman mode of ultrahard fullerite on the pressure following the procedure described in ref 8 using the relation

$$\gamma_i = -\frac{\partial \ln \omega_i}{\partial \ln V} = \frac{B_0}{\omega_0} \frac{\partial \omega_i}{\partial P} \quad (1)$$

where  $\gamma_i$  is the Gruneisen parameter for a quasiharmonic mode of frequency  $\omega_i$  ( $\omega_0$  marks one at a zero pressure).

According to the procedure,<sup>15</sup> the dependencies are replotted in coordinates of relative Raman pressure-induced shifts  $(\omega - \omega_0)/\omega_0$  (here  $\omega$  is the mode frequency of the sample under pressure,  $\omega_0$  is the mode at ambient conditions) against the relative diamond Raman pressure-induced shift of the centroid (determined by a singlet and a doublet mode of the stressed diamond anvil in the diamond pressure scale procedure<sup>16</sup>). Using relation 1, we obtain the bulk modulus of the sample in relation to the bulk modulus of diamond from a dependence slope in the relative coordinates (see Figure 2d). The resulted bulk modulus calculated by this procedure is around 585 GPa in exact agreement to our previous results,<sup>8</sup> where the ultrahard fullerite sample ploughed a diamond anvil during the sample rotation, which is only possible in the case when the hardness of the sample ploughing a diamond exceeds the diamond hardness.

We studied the elastic properties of the proposed nanocomposites model with different sizes of grains and thicknesses of the surrounding diamond matrix shell. Grain sizes change from  $1 \times 1 \times 1$  (0.95 nm) to  $4 \times 4 \times 4$  (3.61 nm) fullerite supercells, while the thickness of a diamond shell varies from 0.70 to 4.70 nm (see the example of the  $2 \times 2 \times 2$  fullerite supercell embedded in the diamond shell with a 1.42 nm thickness presented in Figure 1a). The maximum size of the grain in the model corresponds with the observed size of  $\sim 6$  nm of the experimental superhard sample (Figure 2a).

For the estimation of the compression rate at which the stiffness of the nanocomposite is maximal, we investigated the nanocomposite with a fullerene grain consisting of a  $4 \times 4 \times 4$  (3.61 nm) fullerite supercell with a 1.05 nm thickness of a diamond matrix shell in a wide compression range from 0% to 45% corresponding to the compression of 0 and 108 GPa, respectively. It was found (Figure 3a) that the bulk modulus increases from 345 GPa (0% compression, 0 GPa) to 1450 GPa (27% compression, 56 GPa), and then drops due to the collapsing and losing their intrinsic regular atomic structure (Figure 3b). The critical pressure of amorphization of a fullerite grain corresponds well with the reference data for breaking of a fullerite polymer at the pressure exceeding 40 GPa.<sup>17</sup> We can conclude that at the compression of 27% for this pressure, the stiffest nanocomposite can be formed. In the interface between the fullerite grain and the diamond matrix, a thin layer of  $sp^2$  amorphous carbon with bond lengths from 1.32 to 1.56 Å was formed.

Further, we investigated the dependence of the bulk modulus of the nanocomposite on the diamond matrix shell thickness for the different fullerite grain sizes (Figure 3b) with this value of compression. In the case of the above-considered structure (a  $4 \times 4 \times 4$  fullerite supercell, 3.61 nm) the bulk modulus augmentation rate is the highest in the calculated dependences (red curve), the structures with smaller grains display lower  $B_0$  values. The nanocomposite with a  $4 \times 4 \times 4$  fullerite supercell grain size displays a gradual dependence of the bulk modulus on the thickness of the diamond matrix shell. The bulk modulus rises from  $1100 \pm 174.61 \text{ GPa}$  at the 0.70 nm thickness of the diamond layer and reaches a plateau where the highest value of bulk modulus is  $1712.12 \pm 255.98 \text{ GPa}$  until the diamond layer thickness approaches 3.24 nm.

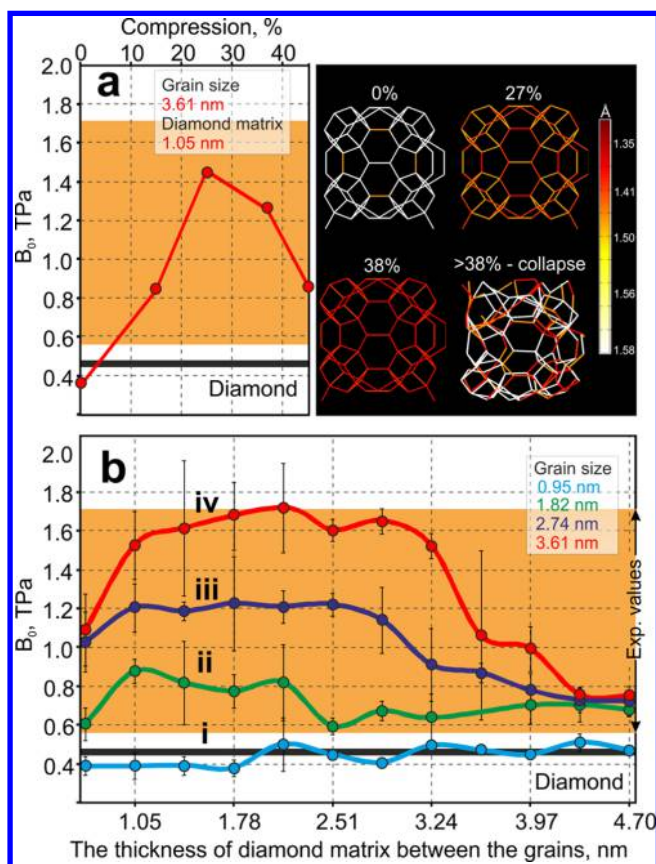


**Figure 3.** (a) The bulk modulus of a nanocomposite containing  $4 \times 4 \times 4$  O’Keeffe fullerite supercell grain (3.61 nm) surrounded by a diamond matrix with a 1.05 nm thickness depending on the amount of fullerite compression. At the right panel, the color distributions of bond length for a fullerene unit of the fullerite grain for different compression rates are shown; (b) the dependence of bulk modulus of a carbon nanocomposite on the thickness of a diamond matrix between the fullerite grains compressed at 27% where the grain sizes equal to (i) 0.95 nm (blue), (ii) 1.82 nm (green), (iii) 2.74 nm (dark blue), and (iv) 3.61 nm (red). The range of experimental values of the bulk modulus from 540 to 1700 GPa<sup>2,8</sup> is denoted by orange.

Similar behavior is observed for the cases of nanocomposites with a grain size of a  $3 \times 3 \times 3$  fullerite supercell (2.74 nm, dark blue) where the value of the bulk modulus reaches plateau at

$1198.6 \pm 123.88$  GPa until the diamond layer thickness approaches 2.88 nm.

Carbon nanocomposite with the grain size of  $2 \times 2 \times 2$  fullerite supercell (1.82 nm) still displays an increased bulk modulus exceeding the diamond value (green). When the diamond matrix shell thickness lies within a range from 1.05 to 2.15 nm, the bulk modulus reaches a plateau at a value of  $871.6 \pm 61.6$  GPa. Further increase of the diamond matrix thickness leads to a smooth reduction of bulk modulus.

The bulk modulus of the structure with the smallest grain (a fullerite unit cell, 0.95 nm) does not display a pronounced dependence on the thickness of a diamond matrix shell and oscillates around the diamond bulk modulus value (457 GPa). Thus, the unit cell of a fullerite grain (Figure 3b) gives only small perturbations within the error, despite of the fact that the fullerite grain is in a compressed state. Therefore, a separate C<sub>60</sub> fullerene in the diamond matrix can be considered only as a 0D defect in the system which does not affect the mechanical characteristics of the whole material.

Also, we found that the increasing size of the fullerite supercell in the grain (more than  $4 \times 4 \times 4$ ) would not lead to a further rising of the bulk modulus due to the decreasing impact of the size effects, and the bulk modulus became practically equal to the  $B_0$  of bulk fullerite under the same strain (in the inset of Figure 1b marked by vertical dotted line). Thus, the calculated bulk modulus of the nanocomposite with the fullerite grains compressed at 27% depending on the grain size (0.95, 1.82, 2.74, 3.61 and 4.55 nm) displays a great augmentation of bulk modulus compared to a single-crystal diamond. Note that the obtained augmented  $B_0$  values is located in the experimental data range<sup>2,8</sup> marked by orange in Figure 3a,b.

In the next part of the paper, we explain the ultrastiff nature of the studied structures. To understand the origin of such effect, we computed a bond length color distribution in the proposed fullerite models as shown in Figure 4a. The fullerite grains are constrained by a diamond matrix which prevents the restoration of the initial relaxed state and promotes the preservation of the compressed state with higher mechanical characteristics. A highly compressed fullerite grain has shortened bonds compared to the diamond matrix. The relatively short bonds will lead to higher stiffness of the grain due to the compression which leads to augmentation of stiffness of the whole nanocomposite.

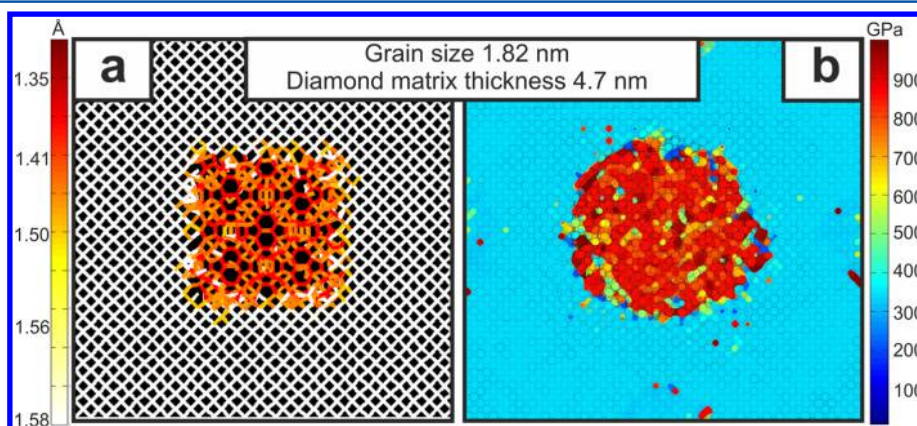


**Figure 4.** (a) Color distribution of bond lengths from 0.135 nm (red color) to 0.158 nm (white color). (b) A map of atom-projected bulk moduli of the nanocomposite with a 1.82 nm grain size and a diamond matrix thickness of 4.7 nm.

For a more detailed investigation of the influence of local rigidity of the grains compared to the diamond matrix, the concept of atomic bulk modulus developed by Kleououlou et al.<sup>18</sup> was applied. Such approach was used in further theoretical work<sup>19</sup> where the investigation of local rigidity in silicon nanocrystals was performed. The validity of this approach application for the proposed fullerite-based nanocomposites is justified by the localized character of C–C bonds. It allows associating the individual stiffness constant and more or less isotropy of the diamond environment at the local level with every bond. The total energy of the system was decomposed into atomic energies  $E_{\text{total}} = \sum_{i=1}^n e_i$  according to the applied approach. The local bulk modulus of each atom shows the contribution of a certain atom to the total rigidity of the nanocomposite and can be defined as

$$B_0^i = V_i \frac{d^2 e_i}{dV_i^2} \quad (2)$$

where  $V_i$  is the Wigner–Seitz atomic volume,  $e_i$  is the energy of each atom in the nanocomposite. Using the values of  $B_0^i$ , the total bulk modulus  $B_0$  of the nanocomposite could be found as the normalized sums over the atomic bulk moduli.

We computed a map of atom-projected bulk moduli of the nanocomposite with a grain size of  $2 \times 2 \times 2$  fullerite supercell (1.82 nm) and the diamond matrix thickness of 4.7 nm, which displays a bulk modulus of  $770.5 \pm 86.6$  GPa, as shown in Figure 4b. It can be seen in Figure 4b that the compressed fullerite grain exhibits a significantly higher bulk modulus marked by red compared to the diamond region marked by blue, which is almost homogeneous and displays the value close to the value of bulk diamond. Inhomogeneous color distribution of the grain region shows that there are parts of fullerite grain (close to the fullerite-diamond interface), which are significantly distorted by the compression. Such regions exhibit high values of bulk modulus, 2 times higher than the bulk modulus of diamond. High values of bulk modulus in the center of the nanocomposite are consistent with the distribution of interatomic bonds shown in Figure 4a; the compressed region corresponds to the more rigid region and vice versa. The obtained results and the computed map of atom-projected bulk moduli of the nanocomposite allow the conclusion that ultra-incompressibility is originated from the mechanical stresses caused by the fullerite grain compression. The extremely high bulk modulus of the central region promotes the augmentation of mechanical characteristics of the whole nanocomposite.

We proposed a model of a fullerite-based nanocomposite where the compressed fullerite grain is incorporated into a diamond matrix, which is consistent with the experimentally obtained ultrahard amorphous carbon. The atomic structure of such complicated systems was investigated in details. The bulk modulus of the nanocomposites depending on the thickness of a diamond matrix between the fullerite grains and on the grain sizes was determined. We observed a great augmentation of the bulk modulus from 590.45 to 1712.12 GPa, which is in a good agreement with experimental data. We plotted the distribution of the interatomic bond lengths to show that the fullerite grain in the nanocomposite is compressed, which leads to an increase in the grain rigidity compared to the diamond environment. To confirm such fact, a map of atom-projected bulk moduli of the nanocomposite with a 1.82 nm grain size and a 4.7 nm diamond matrix thickness was computed. The calculated map

shows that the key to ultra-incompressibility lies in the compressed fullerite grain displaying enhanced bulk modulus (twice bigger!) with respect to bulk diamond.

For a theoretical study of the atomic structure and mechanical properties of the proposed models of the carbon nanocomposite, the empirical many-body Brenner potential<sup>20</sup> was used (implemented into a LAMMPS package<sup>21</sup>) which allows the consideration of systems consisting from thousands to millions of atoms. The undoubted advantage of this method is the possibility of modeling a large system with sufficiently high calculating speed. To achieve a better relaxation of the structure, the simulation of annealing at temperature decreasing from 500 to 10 K was applied, while the maximum interatomic forces became less or equal to 0.05 eV/Å. To evaluate the accuracy of the chosen approach, the cell parameters and elastic properties of bulk diamond and bulk O’Keeffe’s fullerite<sup>12</sup> were calculated. Whereas potential parametrization allows one to predict the structural parameters of bulk diamond with an error less than 0.3% (compared to the experimental data taken from ref 22.:  $a_{\text{calc}} = 3.557$  Å,  $a_{\text{exp}} = 3.568$  Å) the cell parameter of bulk O’Keeffe fullerite also can be estimated with very good accuracy (compared to the density functional theory (DFT) data taken from ref 7.:  $a_{\text{calc}} = 9.77$  Å,  $a_{\text{DFT}} = 9.73$  Å). The bulk modulus of diamond was determined as  $B_0 = 457$  GPa which corresponds well with the experimental values of 445 GPa<sup>8</sup> and 442 GPa.<sup>9</sup> The estimated bulk modulus value of O’Keeffe fullerite equaled 326.6 GPa compared to the theoretical reference data of 369.7 GPa.<sup>4</sup> To evaluate the value of bulk modulus of considered nanocomposites, we performed five computational tests for each structure.

High-pressure experiments were performed using a shear diamond anvil cell (SDAC). The samples were loaded in a steel gasket without a pressure medium. In a SDAC, a controlled shear deformation is applied to the sample under load by rotation of one of the anvils around the anvil’s symmetry axis.<sup>8</sup> The pressure (more precisely, a normal stress component in the sample) was measured from the stress-induced shifts of Raman spectra from the diamond anvil.<sup>16</sup> The purity of C<sub>60</sub> fullerenes used in the study was better than 99.9%. The Raman spectra were recorded with a TRIAX 552 (Jobin Yvon) spectrometer equipped with a CCD Spec-10, 2KBVU Princeton Instruments 2048 × 512 detector and razor edge filters. A transmission electron microscope (TEM) study was done by a JEM 2010 high-resolution microscope.

## ■ AUTHOR INFORMATION

### Corresponding Author

\*E-mail: pbsorokin@tisnum.ru.

### Notes

The authors declare no competing financial interest.

## ■ ACKNOWLEDGMENTS

This work was supported by the Ministry of Education and Science of the Russian Federation, basic program for the National University of Science and Technology MISIS and grant 14.S77.21.0094 (project ID RFMEFI57714X0094). P.B.S. acknowledges the Grant of President of Russian Federation for government support of young PhD scientists MK-6218.2015.2 (project ID 14.Z56.15.6218-MK). The work was done using the Shared-Use Equipment Center of the Technological Institute for Superhard and Novel Carbon Materials. Authors are grateful to the “Chebyshev” and “Lomonosov” super-

computers of the Moscow State University for the possibility of using a cluster computer for our quantum-chemical calculations. Part of the calculations was made on the Joint Supercomputer Center of the Russian Academy of Sciences. The authors thank Prof. Yury Gogotsi and Prof. Vasili Perebeinos for fruitful discussions.

## REFERENCES

- (1) Wang, L.; Liu, B.; Li, H.; Yang, W.; Ding, Y.; Sinogeikin, S. V.; Meng, Y.; Liu, Z.; Zeng, X. C.; Mao, W. L. Long-Range Ordered Carbon Clusters: a Crystalline Material with Amorphous Building Blocks. *Science* **2012**, *337*, 825–828.
- (2) Blank, V.; Buga, S.; Serebryanaya, N.; Dubitsky, G.; Mavrin, B.; Popov, M.; Bagramov, R.; Prokhorov, V.; Sulyanov, S.; Kulnitskiy, B.; et al. Structures and Physical Properties of Superhard and Ultrahard 3D Polymerized Fullerites Created from Solid C<sub>60</sub> by High Pressure High Temperature Treatment. *Carbon* **1998**, *36*, 665–670.
- (3) Okada, S.; Saito, S.; Oshiyama, A. New Metallic Crystalline Carbon: Three Dimensionally Polymerized C<sub>60</sub> Fullerite. *Phys. Rev. Lett.* **1999**, *83*, 1986–1989.
- (4) Berber, S.; Osawa, E.; Tománek, D. Rigid Crystalline Phases of Polymerized Fullerenes. *Phys. Rev. B* **2004**, *70*, 085417.
- (5) Burgos, E.; Halac, E.; Weht, R.; Bonadeo, H.; Artacho, E.; Ordejón, P. New Superhard Phases for Three-Dimensional C<sub>60</sub>-based Fullerites. *Phys. Rev. Lett.* **2000**, *85*, 2328–2331.
- (6) Yang, J.; Tse, J. S.; Iitaka, T. First-principles Investigation on the Geometry and Electronic Structure of the Three-dimensional Cuboidal C<sub>60</sub> Polymer. *J. Chem. Phys.* **2007**, *127*, 134906.
- (7) Perottoni, C. A.; da Jornada, J. A. H. First-principles Calculation of the Structure and Elastic Properties of a 3D-polymerized Fullerite. *Phys. Rev. B* **2002**, *65*, 224208.
- (8) Popov, M.; Kulnitskiy, B.; Blank, V. Superhard Materials Based on Fullerenes and Nanotubes. *Comprehensive Hard Materials*; Elsevier Ltd: Oxford, U.K., 2014, *3*, 515–538.
- (9) Cohen, M. L. Calculation of Bulk Moduli of Diamond and Zincblende Solids. *Phys. Rev. B* **1985**, *32*, 7988–7991.
- (10) Chernozatonskii, L.; Serebryanaya, N.; Mavrin, B. The Superhard Crystalline Three-Dimensional Polymerized C<sub>60</sub> Phase. *Chem. Phys. Lett.* **1999**, *316*, 199–204.
- (11) Murnaghan, F. D. The Compressibility of Media Under Extreme Pressures. *Proc. Natl. Acad. Sci. U.S.A.* **1944**, *30*, 244–247.
- (12) O’Keeffe, M. C<sub>60</sub> Zeolites? *Nature* **1991**, *352*, 674.
- (13) Knudson, M.; Desjarlais, M.; Dolan, D. Shock-wave Exploration of the High-pressure Phases of Carbon. *Science* **2008**, *322*, 1822–1825.
- (14) Brazhkin, V. V.; Lyapin, A. G.; Voloshin, R. N.; Popova, S. V.; Klyuev, Y. A.; Naletov, A. M.; Bayliss, S. C.; Sapelkin, A. V. Mechanism of the Formation of a Diamond Nanocomposite During Transformations of C<sub>60</sub> Fullerite at High Pressure. *JETP Lett.* **1999**, *69*, 869–875.
- (15) Popov, M.; Mordkovich, V.; Perfilov, S.; Kirichenko, A.; Kulnitskiy, B.; Perezhogin, I.; Blank, V. Synthesis of Ultrahard Fullerite with a Catalytic 3D Polymerization Reaction of C<sub>60</sub>. *Carbon* **2014**, *76*, 250–256.
- (16) Popov, M. Pressure Measurements from Raman Spectra of Stressed Diamond Anvils. *J. Appl. Phys.* **2004**, *95*, 5509–5514.
- (17) Moseler, M.; Riedel, H.; Gumbsch, P.; Stäring, J.; Mehlig, B. Understanding of the Phase Transformation from Fullerite to Amorphous Carbon at the Microscopic Level. *Phys. Rev. Lett.* **2005**, *94*, 165503.
- (18) Kleovoulou, K.; Kelires, P. C. Stress State of Embedded Si Nanocrystals. *Phys. Rev. B* **2013**, *88*, 085424.
- (19) Kleovoulou, K.; Kelires, P. C. Local Rigidity and Physical Trends in Embedded Si Nanocrystals. *Phys. Rev. B* **2013**, *88*, 245202.
- (20) Brenner, D. W.; Shenderova, O. A.; Harrison, J. A.; Stuart, S. J.; Ni, B.; Sinnott, S. B. A Second-generation Reactive Empirical Bond Order (REBO) Potential Energy Expression for Hydrocarbons. *J. Phys.: Condens. Matter* **2002**, *14*, 783–802.
- (21) Plimpton, S. Fast Parallel Algorithms for Short-range Molecular Dynamics. *J. Comput. Phys.* **1995**, *117*, 1–19.
- (22) Blank, V.; Aksenenkov, V.; Popov, M.; Perfilov, S.; Kulnitskiy, B.; Tatyani, Y.; Zhigalina, O.; Mavrin, B.; Denisov, V.; Ivlev, A.; et al. A New Carbon Structure Formed at MeV Neutron Irradiation of Diamond: Structural and Spectroscopic Investigations. *Diamond Relat. Mater.* **1999**, *8*, 1285–1290.